Respiratory Commensal Bacteria Reduce the Immune Damage Caused by Influenza Virus Infection by Regulating the Polarization State of Alveolar Macrophages

Liang Chen
Beijing Jishuitan Hospital https://orcid.org/0000-0002-3147-5688
Limei Zhu
Jiangsu Province Center for Disease Control and Prevention
Ying Qi (qiying2021@yeah.net)
Beijing Jishuitan Hospital

Research

Keywords: Influenza, S.aureus, Alveolar macrophage, Cholinergic anti-inflammatory pathway, GTS-21, HMGB1

Posted Date: April 13th, 2021

DOI: https://doi.org/10.21203/rs.3.rs-408345/v1

Abstract

Background

The Role of respiratory tract commensal bacteria in maintaining the immune homeostasis of the respiratory tract is not well eluciated. We aimed to analyze the effect of respiratory symbiotic bacteria on respiratory immune system and its immune response to exogenous pathogens.

Methods

In this study, SPF C57BL/6 male mice were sensitized by nasal drip of respiratory tract symbiotic bacteria *s. aurcus* for 6-8 weeks and then used to establish a *s. aureus* upper respiratory tract symbiosis mouse model. Subsequently, the mice were infected with influenza virus through nasal drip to establish a virus infection model. During the experiment, the immunopathological damage, cytokines and mechanisms related to immune response were analyzed and studied.

Results

The study found that in the *s.aureus* upper respiratory tract symbiosis mouse model, *s.aurcus* sensitization significantly reduced the immune damage in the lungs caused by influenza virus A (IVA) infection, but this protective effect was significantly weakened when alveolar macrophages were cleared. Further studies found that during influenza virus infection, M2 alveolar macrophages (AM) secreted regulatory cytokines to suppress the excessive immune response induced by influenza virus infection. α7nAChR agonist GTS-21 could reduce inflammation in lung tissues, the amount of AM and the expression of inflammatory factors, and the secretion and expression of high-mobility group box 1 (HMGB1) in lung tissues, plasma and bronchoalveolar lavage fluid (BALF). GTS-21 also reduced the lung injury caused by IVA in mice and the levels of M1 type AM bioactive molecules inducible NO synthase (iNOS) and pro-inflammatory factors in AM, and increased the levels of M2 type AM bioactive molecules Arg1 and Ym1. Anti-HMGB 1 antibody reduced the inflammation of lung tissues of mice caused by IVA and inhibited the polarization of AM to M1. Recombinant HMGB1 (rHMGB1) increased the inflammation of lung tissues of mice caused by IVA and promoted the polarization of AM to M1.

Conclusions

Respiratory commensal bacteria induced M2 alveolar macrophages with immunomodulatory function to protect the host against illness and death caused by IVA infection.

Background

The occurrence of infection events will change the microenvironment and homeostasis of the lungs for a long period of time. Therefore, the previous infection events will inevitably affect the subsequent infection events. In the natural state, the human upper respiratory tract is the same as the intestinal tract, with a large number of commensal bacteria [1,2]. During the breathing process, the symbiotic bacteria can enter

the alveolar environment of the lower respiratory tract via air. When this process occurs, in order to maintain the aseptic state of the lower respiratory tract, the body's immune system will generate an immune response against the entered symbiotic bacteria [3,4] to clear the bacteria. Therefore, the immune response of the respiratory immune system to symbiotic bacteria is likely to affect the immune response to other foreign pathogens [5-7]. Studies have found that intestinal commensal bacteria play an important role in maintaining intestinal immune homeostasis and preventing intestinal immune damage and subsequent death [8-10]. However, whether respiratory tract commensal bacteria have functions similar to those of intestinal commensal bacteria in maintaining the immune homeostasis of the respiratory tract is not well known.

S.aureus is a strain of relatively common upper respiratory tract symbiotic bacteria. 25%-50% of the population have *S.aureus* in their upper respiratory tract. At the same time, *S.aureus* is also one of the main participants in secondary bacterial infections induced by influenza virus infection. In this paper, the influence of *S.aureus* respiratory tract pre-sensitization on subsequent IVA infection and its specific immunological mechanism were studied to explore the immunoregulatory effect of macrophage polarity.

Methods

Animal models

Respiratory infection was used to infect mice, and the mice were anesthetized with sodium pentobarbital (50mg/kg). After the mice were in a coma and in an abdominal breathing state, they were instilled via the nose. The nasal drops were used to infect 1500 PFU of H1N1 PR8 strain, and phosphate-buffered saline (PBS) nasal drops were used as a negative control. Each mouse was given 30 ul of nasal drops when the mouse head faced upward and slightly backward. A 50 ul pipette was used to drop the virus into the nostrils of the mouse, and the speed and time interval of instillation were controlled to ensure that the drug completely entered the nasal cavity.

Removal of mouse alveolar macrophages

In order to remove alveolar macrophages from the lung tissues, 30 codronates encapsulated liposomes (CL2MDP) (Annheim, Germany) were injected into the airway every day for 3 days before the mouse influenza model was established. In the control group, equal doses of empty liposomes were given to the airways instead of CL2MDP.

Mouse body weight determination

The body weight of each mouse was measured before viral challenge and on days 1, 3, 5, 7, 9 and 11 of viral challenge. The body weight measuring time was the same on each day. After the measurement, the average weight of each group was calculated and compared with the average weight before challenge to draw a graph.

Serum preparation

The collected whole blood was placed in a 37°C incubator for 1 hour to coagulate, and then placed at 4°C for 0.5 hour to allow the serum to precipitate naturally. After 10 min of centrifugation at 4°C and 3,500 rpm, the serum was gently aspirated into a centrifuge tube and stored frozen at -20°C for later use.

BLAF collection of mouse lung lavage fluid

After the mice were killed by taking blood from the eyeballs, the mouse limbs were fixed, the skin and muscles of the larynx were cut, and the trachea was separated. 4 groups of silk threads were inserted, the abdominal cavity was opened, and the pleural membrane was punctured. Scissors were used to cut a small opening in the trachea. A 19# straight indwelling needle was inserted from the trachea of the larynx and then pulled out to ligate with the silk thread. A 1.0 ml syringe was used to draw 0.8 ml of PBS solution and slowly push it into the lungs. After the lungs were inflated, the lavage fluid was drawn out after a few seconds and this step was repeated 4 times to obtain about 3.0 ml of lung lavage fluid, which was centrifuged at 5,000 rpm and 4°C for 10 min, and 300 ul were taken to detect the protein concentration in the lung lavage fluid, which was then frozen at -80°C after aliquot.

Viral load determination

The instructions of the AgPath-IDTM One-Step RT-PCR Kit (4387424, LIFE, USA) were followed to prepare a fluorescence reverse transcription polymerase chain reaction (RT-PCR) reaction system: 12.5uL of 2×RT-PCR, 1uL of enzyme mixture, 1uL of 10 uM pH1N1-FP and 1uL of pH1N1-RP, 1uL of 5uM pH1N1-Pb, 2.5uL of nuclease-free water, and 5uL of RNA template. The PCR reaction program was set to: 45°C for 30 min; 95°C for 10 min; 95°C for 10 s, 60°C for 30 s, 40 cycles; the fluorescence signal was set to 60°C.

Polarized culture of M1 and M2 alveolar macrophages in vitro

In vitro culture of AM, lipopolysaccharides (LPS) 1ug/ml and interferon-γ (IFN-γ) (Friesoythe, Germany) 20 ng/ml were added to the medium to stimulate AM for 72 hours so they polarized to the M1 type. The application of interleukin-4 (IL-4) (Friesoythe, Germany) 20 ng/ml and IL-13 20 ng/ml for 72 hours polarized the original AMs to the M2 type.

Pathological examination

The prepared tissue sections were stained using the Hematoxylin-Eosin (HE) (Baso, China) staining method: after dewaxing, benzene removal, rehydration, staining with hematoxylin and eosin, dehydration, transparency treatment, and mounting and fixing, the tissue sections were stained by HE. Histopathological observation and analysis were performed under an optical microscope. After staining, the nucleus was blue-purple, and the cytoplasm was red.

Lung wet/dry ratio (W/D)

After the left lung of the mouse was obtained, the residual blood was washed away with cold normal saline. The filter paper was used to absorb residual water, and the lung was accurately weighed on a

micro scale to obtain the "wet" weight of the lung. Then, the specimen was placed in an oven at 80°C, and the lung tissue was taken out after 48 hours. The lungs were heavily "dry" at this moment. Each lung tissue was placed on a tin foil and weighed together with the tin foil. After labeling, the lung tissue was put in the oven to dry, and then the dry weight was weighed after the weight became stable. Finally, the weight of the tin foil was subtracted to calculate the wet to dry weight ratio, which reflected the degree of lung tissue edema.

Determination of myeloperoxidase (MPO) activity in lung tissues

First, the mouse lung tissue was fully ground in PBS with a homogenizer to obtain 10% lung tissue homogenate. Then, following the specific steps in MPO kit instructions (Nanjing Jiancheng, China) , a spectrophotometer was used to measure the optical density at 450 nm. The MPO level in the lung tissue was calculated according to the standard and was expressed in u/g.

Determination of cytokine levels

The enzyme-linked immunosorbent assay (ELISA) method was used to determine the levels of cytokines. The cytokines measured in this part were TNF-α, IL-1β, IL-6, and monocyte chemoattractant protein-1 (MCP-1). All operating methods were performed in accordance with the instructions of the ELISA kit (Hangzhou Lianke, China).

Flow cytometry

After a single cell suspension of mononuclear cells (MNCs) in left mouse lung (concentration, 2×10^6/m1) was obtained, a certain amount of phycoerythrin E (phycoerythrin, PE) labeled CDllc antibody (eBioscience, USA) and allophycocyanin 7 (Allophycocyanin 7) was added according to the antibody instructions. Allophycocyanin-cyanin7 (APC-Cy7) labeled F4/80 antibody (Biolegend, USA) was used to stain and label AM, which was vortexed and mixed well before being stained for 60min at 4℃ in the dark. AM was labeled as F4/80 and CD11 double positive cells. Then, the cells were washed once with 2ml of PBS and resuspended with 100ul of PBS. Fluorescein isothiocyanate (FITC) (eBioscience, USA), CD206 (eBioscience, USA), Allophycocyanin (APC)-iNOS (Biolegend, USA), FITC-IL-10 (eBioscience, USA), FITC-IL-6 (eBioscience, USA) and APC-IL-12p40 (eBioscience, USA) antibodies were then added for the second time of staining at 4°C for 60 min in the dark. Before staining, the cells re-stained with APC-iNOS, FITC-IL-10, FITC-IL-6 and APC-IL-12p40 antibodies should be stained with an equal volume of fixative, and the cells were fixed at room temperature in the dark for 30 minutes. Then, each tube was added with the 1×membrane breaking agent for membrane breaking treatment. After the staining step, the cells were washed with 2ml of PBS once again, and finally resuspended with 300ul of PBS before testing on the machine. The expression ratio of iNOS+, CD206+, IL-10+, IL-6+ and IL-12p40+ in F4/80+CD11c+MNCs(AM) was analyzed. Among them, F4/80+CD11C+iNOS+MNCs were M1 type AMs, and F4/80+CD11c+CD206+MNCs were M2 type AMs. FlowJo software was used to analyze the results.

Preparation and culture of bone marrow-derived macrophage cells (BMMCs)

Female C57BL/6 mice were sacrificed by cervical spine dislocation. The head was soaked and disinfected in 75% alcohol for 15 minutes. The lower limbs of the mouse were cut with sterile scissors. The skin and muscle tissues were separated layer by layer, and the skin and muscle were separated using tissue scissors and forceps. The separated femur and tibia of the lower limbs of the mouse were placed in PBS containing 5% double antibiotics (penicillin/streptomycin, 100×), transferred to a clean bench, washed again with PBS containing 5% double antibiotics, and then transferred to a 10 cm Petri dish with PBS containing 5% double antibiotics. The muscle tissues on the femur and tibia were thoroughly removed and put in a Petri dish, the femur and tibia were separated, and the tissues were transferred to a 6-well plate. Sterile scissors were used to cut both ends off the bone shaft, a 1ml syringe was used to draw some RPMI 1640 medium, and the bone marrow was flushed into the other side of the 6-well plate. The mouse bone marrow cell suspension in the culture dish was collected for low-temperature centrifugation (1500rpm×7min, 4℃). After centrifugation, the supernatant was discarded, red blood cells were removed with a red blood cell lysate, and the cells were resuspended in RPMI 1640 complete medium (containing 10% FBS and 1% double antibiotics) and counted. The cells were placed in a 37°C, 5% CO_2 incubator for 4 hours to collect non-adherent cells. RPMI 1640 complete medium was used to adjust the cell suspension concentration to 2×10^6/ml in a total volume of 10ml, and recombinant mouse interleukin 4 (rmIL-4) 10ng/m1 and macrophage colony-stimulating factor (M-CSF) 10ng/m1 were added to induce differentiation. The cells were incubated in an incubator at 37℃ and 5% CO_2 for 7 days, and half of the medium was changed every other day. All BMMCs were collected on day 7.

Statistical processing

Statistical analysis was conducted using SPSS 22.0 statistical software. Measurement data with a normal distribution and uniform variance were expressed as mean ± standard deviation ($\bar{x} \pm s$), and the univariate analysis of variance or repeated measurements was used to compare multiple groups of means. The LSD-t test was used for further pairwise comparison. $P < 0.05$ was considered statistically significant.

Results

Respiratory symbiotic bacteria reduced the infection ability of IVA

The mice began to show clinical symptoms on the 3rd day, mainly manifested as arched back, curled up body, trembling, poor reaction activity, reduced activity, and listlessness. In the normal control group, the mice had a shiny fur, sensitive response, normal diet, active activities, and weight gain. The weight of the mice in the IVA group began to gradually decrease. On the 5th day after infection, the symptoms worsened, and the mice showed obvious weight loss, decreased body temperature, shortness of breath, closed eyes, and death (Fig 1.A).

Virus infection caused significant differences in the survival rate of mice, and IVA infection killed about 43% of the mice. The mice in the IVA+ symbiotic bacteria group (IVA+SB group) also died 7-9 days after

infection. The weight of the mice that were still alive 9 days later slowly recovered, and no more deaths occurred. Some mice in the IVA + symbiotic bacteria + macrophage removal group (IVA+SB+MR group) also died on the 7th day after infection, with a mortality rate of 50%. By the 11th day after infection, all mice in the IVA group and the IVA+SB+MR group died (Fig 1.B).

H&E staining of lung tissues showed that compared with the control group after IVA infection, the mice in the other groups all showed pulmonary inflammation, inflammatory cell infiltration in the lungs, large number of inflammatory cells gathered in alveolar cavity, and protein-rich tissue fluid extravasated to the alveolar cavity. The survival mice in the IVA+SB group had milder lung inflammation and their alveolar structure tended to be intact. In the lungs of the two groups of mice dying after infection, their alveolar structure collapsed with the formation of hyaline membranes. Pulmonary interstitial swelling and congestion, telangiectasia, and extravasation indicated that the lung pathology of the mice in the IVA group and the IVA+SB+MR group became worse after IAV infection, and their lungs were severely damaged (Fig 1.C).

Further analysis of the pulmonary edema in the lungs of the mice after infection showed that, except for the control group, the W/D of the lungs of the mice in all other groups was significantly increased after infection. The mice in the IVA group were better than those in the IVA +SB+MR group. The mice in the IVA group were slightly up-regulated, but there was no significant difference (Fig 1.D). This result revealed that the pulmonary edema of the mice in the IVA group and the IVA+SB+MR depletion group was more severe in the later stage of infection.

Analysis of the protein concentration in the alveolar lavage fluid of infected mice showed that the protein content in the alveolar fluid of each group of mice was significantly higher than that of the control group (about 1,000pg/m1) after infection. The protein content of mice in the IVA group and the IVA+SB+MR group even increased to more than 2,000pg/ml. This result indicates that IAV infection caused damage to mouse lung epithelial cells and capillary extravasation (Fig 1.E).

In order to explore whether the severe lung injury in mice was caused by the persistent infection of H1N1 virus, the virus titer in the lung tissue of infected mice was analyzed. As expected, the changes in virus titer in infected mice were consistent. On the third day after infection, except for the control group, the virus titer of mice in all other groups reached high levels (about 10^6 CCID50/ml). On the 5th day after infection, the titer and virus load of the mice in the IVA+SB group began to decrease, and the virus was reduced to less than 10 CCID50/ml 11 days after infection. The virus continued to multiply on the fifth day after infection in the IVA group and the IVA+SB+MR group. On the 9th day after infection, the virus titer and load of the mice in the IVA group and the IVA+SB+MR group began to fall, but virus was still present (Fig 1.F). This result confirmed that compared with the mice in the IVA+SB group, the mice in the IVA+SB+MR group did not effectively clear the H1N1 virus after infection, resulting in a large amount of virus still present in the lungs one week after infection.

The role of M1 and M2 alveolar macrophages in the lung injury caused by IVA infection in the presence of respiratory symbiotic bacteria

To verify the effect of M1 and M2 polarized AMs on the inflammatory infiltration of respiratory commensal bacteria in the lungs of mice infected by influenza virus, clodronate liposomes (CL2MDP) were used to inject AMs into mice by internal injection, and then the M1 or M2 alveolar macrophages differentiated in vitro were transferred to AM-depleted mice through the airway. The mice were divided into the control group, IVA group, IVA+SB group, IVA+SB+MR group, IVA+MR+M1 group, and IVA+MR+M2 group. By measuring the changes of these two indicators in each group, the influence of M1 type AM or M2 type AM on the lung inflammation in mice infected with influenza virus could be further clarified. The results are shown in the figures (Fig 2.A and B). When the IVA+SB+MR group was compared with the IVA+SB group, the W/D and MPO values were significantly higher. The W/D and MPO values of the IVA+MR+M2 group were significantly reduced when compared with the IVA+SB+MR group. The above results indicated that AM was involved in the regulation of pulmonary edema and neutrophil infiltration in influenza-infected mice. M1 type AM could aggravate the degree of pulmonary edema and neutrophil infiltration in mice; M2 type AM could reduce the degree of pulmonary and neutrophil infiltration.

The levels of representative pro-inflammatory factors (TNF-α, IL-1 β, IL-6, MCP-1) in the BALF of each group of mice were also measured to reflect the degree of inflammation in the lung tissues. Compared with the MR group, the levels of TNF-α, IL-6 and IL-1β cytokines secreted by M1-type AM were significantly reduced after AM depletion. The adoptive transfer of M1 type AM significantly increased the levels of TNF-α, IL-6, IL-1β and MCP-1 in BALF of mice after AM was removed. When the IVA+MR+M1 group was compared with the IVA+MR+M2 group, the secretion levels of TNF-α, IL-6, IL-1β, and MCP-1 in BALF were significantly increased. By combining the above W/D and MPO test results, it can be concluded that AM plays an important role in the pathogenesis of lung injury caused by influenza virus (Fig 2.C-F). Among them, M1 type AM participates in aggravating the degree of inflammation in the lung tissues of mice, and M2 type AM exerts an opposite effect.

The cholinergic signal pathway regulated the polarization of AMs in lung injury caused by IVA

In order to determine the effect of GTS-21 on lung inflammation in mice after influenza infection, the MPO of lung tissues, the W/D of the lung, and the expression of inflammatory cytokines in BALF were measured. The results showed that compared with the control group, there was no significant difference in the above indicators in the GTS-21 group, indicating that GTS-21 had no effect on normal mice. After influenza virus infection, GTS-21 intervention was performed. Compared with the influenza virus infection group, the lung MPO activity of mice was significantly reduced, and the W/D ratio was also significantly reduced (Fig 3.A and B). By measuring the levels of inflammatory factors (IL-6, IL-1β, TNF-α, MCP-1) in BALF, it was seen that the GTS-21+ influenza virus infection group had a significant decrease compared with the IVA group (Fig 3.C-F). It can be inferred that the intervention of GTS-21 significantly reduced lung inflammation in mice after influenza infection.

Can GTS-21 participate in the treatment of lung injury after IVA infection by regulating AMs? To answer this question, the changes in AM function were measured with or without GTS-21 intervention. First, AMs were isolated from mouse BALF, and CD11+F4/80+ cells were screened out through flow cytometry. Then, by analyzing the changes in the number of AMs after GTS-2l intervention, it was observed whether GTS-2l had an impact on the number of AMs. As shown in the figure, the number of AMs in the IVA group was significantly higher than that in the control group, and after GTS-21 intervention, the number of AMs was significantly lower than that in the non-intervention group (Fig 4.A). In other words, GTS-2l reduced the number of AMs in IVA infected mice. The main inflammatory factors expressed on the surface of AMs were determined by staining: IL-6 and IL-12p40 were pro-inflammatory factors, and IL-10 was an anti-inflammatory factor (Fig 4.B-D). As shown in the figure, the expression levels of IL-6 and IL-12p40 in the IVA+GTS-21 group were significantly lower than those in the IVA group, while the IL-10 expression level was significantly increased. The above results indicated that GTS-21 reduced the number of AMs after lung injury in IVA infected mice, reduced the expression of pro-inflammatory factors IL-6 and IL-12 on the surface of AMs, and increased the expression of anti-inflammatory factor IL-10 on the surface of AMs. This confirmed that one of the anti-inflammatory mechanisms of GTS-21 on lung injury after IVA may be that it reduced the number of AMs, promoted the secretion of anti-inflammatory factor IL-10 by AMs, and inhibited the secretion of pro-inflammatory factors IL-6 and IL-12.

GTS-21 inhibited expression and secretion of HMGB1 by AMs after IVA infection

ELISA was used to verify the effect of GTS-21 on the secretion of HMGB1 by AMs after IVA infection. It was found that the levels of HMGB1 in serum and BALF in the IVA+GTS-21 group were significantly lower than those in the IVA group (Fig 5.A and B). Further measurement of the mRNA level of HMGB1 in the AMs of IVA mice showed that the mRNA level of HMGB1 in the AMs of IVA mice was significantly lower than that of IVA mice without GTS-21 intervention (Fig 5. C). The experimental results showed that GTS-21 reduced the expression of HMGB1 in the AMs of IVA-infected mice, and reduced the concentration and mRNA of HMGB1 in serum, BALF and AMs.

In order to confirm the polarizing effect of GTS-21 on the AM of mice infected by IVA, the AMs extracted from the mouse BALF were first subjected to flow cytometry to screen out CDIIc+F4/80+ AMs. The factors expressed on the surface of murine AMs were determined. The surface of M1-AM expressed the iNOS factor, and the surface of M2-AM expressed the CD206 factor. Therefore, the change in the ratio of iNOS+ to CD206+ AM could reflect the change in the ratio of M 1-AM to M2-AM. The results showed that iNOS+CDIIc+F4/80+ cells represented M1-AM, and CD206+CDIIc+F4/80+ cells represented M2-AM. The proportion of iNOS+CDIIc+F4/80+ cells in the IVA group was significantly higher than that in the control group, but the proportion decreased significantly after GTS-21 intervention (Fig 6.A and B). It was shown that GTS-21 down-regulated the ratio of M1-AM in IVA mice. The ratio of CD206+CDIIc+F4/80+ cells in the IVA group was significantly lower than that in the control group, and the ratio increased significantly after GTS-21 intervention. It was also shown that GTS-21 up-regulated the ratio of M2-AM in IVA mice.

iNOS is a biomarker of M1-AM, and Arg1 and Ym1 are biomarkers of M2-AM. Therefore, by measuring the expression of iNOS, Arg1 and Ym1, the expression of M1-AM and M2-AM can be indirectly reflected. The RT-PCR method was used to determine the mRNA levels of iNOS, Arg1 and Ym1 in the lung tissues of mice. As shown in the figure (Fig 6.C -E), the mRNA expression of iNOS in the lung tissues of the IVA group was significantly higher than that in the control group, while the mRNA levels of Arg1 and Ym1 were significantly lower than those of the control group. It was shown that the AMs of IVA mice was mainly polarized to M1-AMs. The mRNA level of iNOS expressed in mice after GTS-21 intervention was significantly lower than that of IVA mice, while the mRNA expression levels of Arg1 and Ym1 were significantly higher than those of IVA mice. Therefore, the above results suggested that IVA stimulated the polarization of AMs to M1-AMs in mice, and this polarization was weakened by the intervention of GST-21.

HMGB1 regulated the polarization of M1 macrophages in lung injury caused by IVA

In order to study whether HMGB 1 has an effect on the polarization of IVA-induced lung injury in mice, flow cytometry was used to determine the percentage of molecules expressed on AM surface. MHCII, CD80, CD86 and CD40 are surface biomarkers related to M1 type AM. CD206 and IL-10 are surface biomarkers related to M2 type AM. The percentage changes of these surface biomarkers under different interventions of rHMGB1 and anti-HMGB1 can reflect the trend of changes in M1 type AM and M2 type AM. As shown in the figure, compared with the IVA group, the percentages of MHCII+, CD80+, CD86+, and CD40+ cells in the IVA+anti-HMGB1 group decreased significantly, while the percentage of CD206 cells increased significantly, while the percentage of IL-10+ cells did not change significantly. Compared with the IVA group, the percentages of MHC□+, CD80+, CD86+, and CD40+ cells in the IVA+rHMGB1 group increased significantly, while the percentages of CD206+ and IL-10+ cells decreased significantly. This result showed that anti-HMGB1 inhibited the M1 polarization of AMs in mice after IVA infection and promoted the M2 polarization of AMs, while rHMGB1 promoted the M1 polarization of AMs in IVA-infected mice and inhibited the M2 polarization of AMs (Fig 7.A -F). In other words, HMGB1 participated in the generation of inflammatory response after IVA infection by promoting the M1 polarization of AMs and inhibiting the M2 polarization of AMs.

The ELISA method was used to determine the expression of inflammatory factors in the culture supernatant of mouse bone marrow-derived macrophages, and the results could also indirectly reflect the expression of M1 and M2 macrophages. As shown in the figure, the levels of cytokines IL-6, TNF-α, and MCP-1 in the IVA+rHMGB1 group were significantly higher than those in the IVA group, while the level of IL-10 was significantly lower than that in the IVA group; the levels of IL-6, TNF-α, and MCP-1 cytokines in the IVA+anti-HMGB1 group were significantly lower than those of the IVA group, while the level of IL-10 was significantly higher than that of the IVA group (Fig 7.G -J). Therefore, it was confirmed that rHMGB1 up-regulated the level of cytokines associated with M1 macrophages in IVA-infected mice and down-regulated the levels of cytokines associated with M2 macrophages in IVA-infected mice, while Anti-HMGB1 exerted the opposite effects. The results further confirmed that HMGB1 participated in the

generation of inflammatory response in IVA-infected mice by promoting the M1 polarization of macrophages and inhibiting the M2 polarization of macrophages.

Discussion

The respiratory tract symbiotic flora is known as the "gatekeeper" of respiratory health. It plays an important role in organ development and immune homeostasis maintenance, and has precise and specific functions in the regulation of lung immune response. In this research, using a mouse model of H1N1 adapted strains, it was found that the commensal bacteria group had lower mortality after infection, and its lung inflammation and pathological damage in the later stage of infection were also relatively lighter, revealing the role of commensal bacteria in protecting the body against H1N1 virus infection [11,12]. The analysis of virus titer and load found that macrophages were removed and the virus could not be cleared in time and effectively after infection, revealing that the lack of macrophages caused severe viral pneumonia in mice. The analysis also suggested that macrophages affected the body's anti-virus immune response. Through monitoring and analysis of immune cells in the lungs of infected mice, it was found that the number of macrophages was increased in the early stage of infection. A large number of studies have confirmed that macrophages play a key antiviral role in the early stage of viral pneumonia.

Under physiological conditions, the main role of AMs is to remove cell debris from tissues and exert anti-inflammatory effects. However, if the tissue is damaged or invaded by pathogenic microorganisms, AMs will initiate a strong pro-inflammatory response to maintain tissue homeostasis. AMs can serve as antigen-presenting cells to other immune cells and pro-inflammatory cells such as dendritic cells (DC). By participating in the regulation of the body's immune response, AMs can be called the body's sentinel cells that resist external inflammatory stimuli. In studying the role of AMs in influenza infection in the presence of commensal bacteria, the experiments in this study showed that even if the commensal bacteria were still present, the pathological damage of the lung tissue caused by IVA and the lung injury score would increase if AMs were removed from the mice. The degree of pulmonary edema (W/D) was higher than that of the IVA+ symbiotic bacteria group. Lung MPO activity was significantly higher than that of the IVA+ symbiotic bacteria group.

Macrophages can be polarized to the M1 type to mainly strengthen the pro-inflammatory response and the M2 type to initiate tissue repair [13,14]. In different stages of inflammation, the ratio of M1 and M2 type macrophages can change to exert different pro-inflammatory and repair effects [15]. In this experiment, it was verified that AMs also regulated the balance between M1 type and M2 type in mice infected with IVA by respiratory symbiotic bacteria.

By removing AMs from the mice and then adoptively transferring MI type AM and M2 type AM, it was found that compared with the IVA+ symbiotic bacteria mice with AMs removed, the pathological damage to the lung tissue of the M1 type AM adoptive group was increased. Compared with the M1 type AM adoptive group with AMs removed, the pulmonary edema (W/D), the lung MPO activity, and the

expression of inflammatory factors in BALF all increased. This is basically consistent with the results of the pro-inflammatory response of MI type AM. In other words, M1 type AM mainly enhances the inflammatory response during the body's inflammatory response. Compared with the AMs removal group, the M2 type of AM adoptive transfer group had significantly lower lung injury scores, significantly reduced lung edema (W/D), significantly reduced lung MPO activity, and decreased MCP-1 expression in BALF. It can be seen that, in this process, M2 type AM mainly reduces lung damage and promotes tissue repair, which are basically the same as the functions of M2 type AM.

The cholinergic anti-inflammatory pathway regulates cholinergic nerves and their transmitters against systemic inflammation. This pathway can quickly and effectively alleviate inflammation through the vagus nerve. Acetylcholine released from the end of the efferent branch of the vagus nerve can bind to the a7nAchR receptor on macrophages to inhibit the production of pro-inflammatory factors. GTS-21 is a specific agonist of a7nAehR. It can activate the cholinergic anti-inflammatory pathway and bind to a7nAchR on the surface of macrophages to exert anti-inflammatory effects [16]. Therefore, investigation on the interventional effect of GTS-21 on commensal bacteria in the regulation of AMs in lung injury after IVA infection may clarify the anti-inflammatory mechanism of the cholinergic anti-inflammatory pathway and provide an intervention target for the neural anti-inflammatory process of viral pneumonia. This study verified that GTS-21 reduced lung inflammation in IVA-infected mice mainly by reducing pulmonary edema, reducing lung MPO activity, and reducing expression of inflammatory factors in BALF. It was proved from many aspects that GTS-21 had a definite anti-inflammatory effect on lung injury caused by IVA infection. In addition to affecting the number of AMs, GTS-21 may also play anti-inflammatory roles by changing the form and function of AMs. Therefore, through experiments, it was further proved that GTS-21 had a modulating effect on the polarization of AMs in lung injury caused by IVA infection, and GTS-21 indeed participated in the anti-inflammatory process by reducing the number of AMs and adjusting the polarization direction of AMs [17]. The adjustment of the polarization direction of AM by GTS-21 is to inhibit the development of AM in the direction of M1-AM and promote the development of AMs in the direction of M2-AM [18].

In this study, by measuring the concentration of HMGB1 in serum, BALF and AMs ,it was also confirmed that GTS-21 activated a7nAehR and the cholinergic anti-inflammatory pathway, acted on the a7nAehR receptor of AMs, and inhibited the secretion and expression of HMGB1 by AMs, so as to exert an anti-inflammatory effect. In addition, during the inflammatory response, macrophages secrete HMGB1 to interact with other macrophages and to increase the secretion of other pro-inflammatory factors, thereby enhancing the inflammatory response.

Under normal physiological conditions, HMGB1, as a highly conserved protein, exists in most cell nuclei to control gene expression. It is regarded as an important DNA molecular chaperone involved in gene regulation. However, HMGB1 was also discovered as an important alarm element, and the role of HMGB1 in mediating the activation of innate immune response and regulating damage inflammation has received great attention. In an acute lung injury and acute respiratory distress syndrome (ALI/ARDS) study, the level of HMGB1 in the plasma and lung epithelial mesenchymal cells of mice was significantly

increased. HMGB1 can directly cause ALI and acute lung inflammation, damage lung parenchymal cells and increase the release of inflammatory cytokines [19]. Therefore, it is of great significance to use HMGB1 as a research and treatment target for viral pneumonia caused by IVA.

Macrophages, like dendritic cells, act as antigen-presenting cells in the process of innate immune response. They can engulf foreign pathogens and present them to T cells to initiate an immune response. The costimulatory molecules major histocompatibility complex-II (MHC-II), CD80, CD86, CD40 and programmed death-ligand 1 (PD-L1) on the surface of macrophages play an important regulatory role in antigen presentation[20-22]. In this study, the surface molecules of M1 type macrophages, MHC-II, CD80, CD86, and CD40, and the surface molecules of M2 type macrophages, CD206 and IL-10, were measured to reflect the effect of HMGBl on IVA infection in the lungs. The results showed that the expression levels of surface molecules MHC-II, CD80, CD86, and CD40 on M1 macrophages increased significantly after the action of rHMGB1, and decreased significantly after the action of anti-HMGB1 [23,24]. It was shown that HMGB1 promoted the polarization of M1 macrophages after IVA infection. On the other hand, CD206 and IL-10, which represented the surface molecules of M2 macrophages, were significantly reduced after the action of rHMGB1, and the level of CD206 was significantly increased after the action of anti-HMGB1, although the expression level of IL-10 did not change significantly.

In this study, the results suggested that HMGB1 may have an inhibitory effect on the polarization of M2 macrophages after IVA infection. This clarified an important mechanism of HMGBI in macrophage regulation. In the process of lung injury caused by IVA, respiratory commensal bacteria induced down-regulation of HMGB1 to down-regulate inflammation by inhibiting the M1 polarization of macrophages or promoting M2 polarization.

Conclusions

In summary, respiratory symbiotic bacteria can protect the host against lung injury caused by influenza virus infection by inducing the polarization of alveolar macrophages with immunomodulatory functions. Under the induction of symbiotic bacteria, the cholinergic anti-inflammatory pathway can reduce the number of AMs, inhibit the polarization of M1 type AM, and inhibit the secretion of HMGB1 by AMs to reduce the pulmonary inflammation caused by IVA infection.

Declarations

Ethics approval and consent to participate

Not applicable.

Consent for publication

Not applicable.

Competing interests

The authors declare that they have no confict of interest.

Founding

This study was founded by Beijing JST research (ZR-202113).

Data Availability

The data used to support the findings of this study are available from the corresponding author upon request.

Authors' Contributions

Liang Chen designed the study, carried out the test, and drafted the manuscript; Limei Zhu carried out the test and revised the manuscript; Ying Qi designed the study, carried out the test and analyze of data. All authors agree with the article submission. All authors read and approved the final manuscript.

References

1. Paulraj Kanmani, Patricia Clua, Maria G Vizoso-Pinto, Cecilia Rodriguez, Susana Alvarez, Vyacheslav Melnikov, et al. Respiratory Commensal Bacteria Corynebacterium pseudodiphtheriticum Improves Resistance of Infant Mice to Respiratory Syncytial Virus and Streptococcus pneumoniae Superinfection. Front Microbiol. 2017;8:1613. doi: 10.3389/fmicb.2017.01613.
2. Sarah E Clark. Commensal bacteria in the upper respiratory tract regulate susceptibility to infection. Curr Opin Immunol. 2020;66:42-49. doi: 10.1016/j.coi.2020.03.010..
3. Rabia Khan, Fernanda Cristina Petersen, Sudhanshu Shekhar. Commensal Bacteria: An Emerging Player in Defense Against Respiratory Pathogens. Front Immunol. 2019;10:1203. doi: 10.3389/fimmu.2019.01203..
4. Takeshi Ichinohe, Iris K Pang, Yosuke Kumamoto, David R Peaper, John H Ho, Thomas S Murray, et al. Microbiota regulates immune defense against respiratory tract influenza A virus infection. Proc Natl Acad Sci U S A. 2011;108(13):5354-9. doi: 10.1073/pnas.1019378108.
5. Apollo Stacy, Derek Fleming, Richard J Lamont, Kendra P Rumbaugh, Marvin Whiteley. A Commensal Bacterium Promotes Virulence of an Opportunistic Pathogen via Cross-Respiration. mBio. 2016;7(3):e00782-16. doi: 10.1128/mBio.00782-16..
6. Kourosh Honarmand Ebrahimi. SARS-CoV-2 spike glycoprotein-binding proteins expressed by upper respiratory tract bacteria may prevent severe viral infection. FEBS Lett. 2020;594(11):1651-1660. doi: 10.1002/1873-3468.13845..
7. J D Huang, B J Zheng, K Y Yuen. A bioshield against influenza virus infection by commensal bacteria secreting antiviral peptide. Hong Kong medical journal. Hong Kong Med J. 2016;22(3 Suppl 4):13-5.

8. Sha Wu, Zhen-You Jiang, Yi-Fan Sun, Bin Yu, Jia Chen, Cong-Qi Dai, et al. Microbiota Regulates the TLR7 Signaling Pathway Against Respiratory Tract Influenza A Virus Infection. Curr Microbiol. 2013;67(4):414-22. doi: 10.1007/s00284-013-0380-z.
9. Christopher Bandoro, Jonathan A Runstadler. Bacterial Lipopolysaccharide Destabilizes Influenza Viruses. mSphere. 2017;2(5):e00267-17. doi: 10.1128/mSphere.00267-17.
10. Tomoko Nishikawa, Kazufumi Shimizu, Torahiko Tanaka, Kazumichi Kuroda, Tadatoshi Takayama, et al. Bacterial Neuraminidase Rescues Influenza Virus Replication from Inhibition by a Neuraminidase Inhibitor. PLoS One. 2012;7(9):e45371. doi: 10.1371/journal.pone.0045371.
11. Michael C Abt, Lisa C Osborne, Laurel A Monticelli, Travis A Doering, Theresa Alenghat, Gregory F Sonnenberg, et al. Commensal bacteria calibrate the activation threshold of innate antiviral immunity. Immunity. 2012;37(1):158-70. doi: 10.1016/j.immuni.2012.04.011.
12. Hui-Wen Chen, Pei-Feng Liu, Yu-Tsueng Liu, Sherwin Kuo, Xing-Quan Zhang, Robert T Schooley, et al. Nasal Commensal Staphylococcus epidermidis Counteracts Influenza Virus. Sci Rep. 2016;6:27870. doi: 10.1038/srep27870.
13. Jia-Xi Duan, Yong Zhou, Ai-Yuan Zhou, Xin-Xin Guan, Tian Liu, Hui-Hui Yang, et al. Calcitonin gene-related peptide execs anti-inflammatory property through regulating murine macrophages polarization in vitro. Mol Immunol. 2017;91:105-113. doi: 10.1016/j.molimm.2017.08.020.
14. Abbas Shapouri-Moghaddam, Saeed Mohammadian, Hossein Vazini, Mahdi Taghadosi, Seyed-Alireza Esmaeili, Fatemeh Mardani, et al. Macrophage plasticity, polarization, and function in health and disease. J Cell Physiol. 2018;233(9):6425-6440. doi: 10.1002/jcp.26429..
15. Maor Sauler, Yi Zhang, Jin-Na Min, Lin Leng, Peiying Shan, Scott Roberts, et al. Endothelial CD74 mediates macrophage migration inhibitory factorprotection in hyperoxic lung injury. FASEB J. 2015;29(5):1940-9. doi: 10.1096/fj.14-260299.
16. X Yang, C Zhao, X Chen, L Jiang, Xiao Su, et al. Monocytes primed with GTS-21/a7 nAChR (nicotinic acetylcholine receptor) agonist develop anti-inflammatory memory. QJM. 2017;110(7):437-445. doi: 10.1093/qjmed/hcx014.
17. Ravikumar A Sitapara, Alex G Gauthier, Vivek S Patel, Mosi Lin, Michelle Zur, Charles R Ashby Jr, et al. The α7 nicotinic acetylcholine receptor agonist GTS-21 improves bacterial clearance in mice by restoring hyperoxia-compromised macrophage function. Mol Med. 2020;26(1):98. doi: 10.1186/s10020-020-00224-9.
18. Xiao-Jing Wu, Xu-Ming Yang, Xue-Min Song, Yang Xu, Jian-Guo Li, Yan-Lin Wang, et al. The role of erbin in GTS-21 regulating inflammatory responses in MDP-stimulated macrophages. Shock. 2017;47(5):653-657. doi: 10.1097/SHK.0000000000000785..
19. Chan-Ho Lee, Seong-Jin Yoon, Sun-Mee Lee. Chlorogenic acid attenuates high mobility group box 1(HMGB 1) and enhances host defense mechanisms in murine sepsis. Mol Med. 2013;18(1):1437-48. doi: 10.2119/molmed.2012.00279..
20. Chan-Ho Lee, Seong-Jin Yoon, Sun-Mee Lee. Mesenchymalstem cells reciprocally regulate the M1/M2 balance in mouse bone marrow-derived macrophages. Mol Med. 2013;18(1):1437-48. doi:

10.2119/molmed.2012.00279..

21. Huai-Dong Li, Qing-Xiang Zhang, Zhi Mao, Xing-Jie Xu, Nai-Yi Li, Hui Zhang. Exogenous interleukin-10 attenuates hyperoxia-induced acute lung injury in mice. Exp Physiol. 2015;100(3):331-40. doi: 10.1113/expphysiol.2014.083337..
22. Kenta Kambara, Wakana Ohashi, Kengo Tomita, Michinori Takashina, Shiho Fujisaka, Ryuji Hayashi, et al. In vivo depletion of CD206+ M2 macrophages exaggerates lung injury in endotoxemic mice. Am J Pathol. 2015;185(1):162-71. doi: 10.1016/j.ajpath.2014.09.005..
23. S Y Wang, Z J Li, X Wang, W F Li, Z F Lin . Effect of ulinastatin on HMGB 1 expression in rats with acute lung injury induced by sepsis. Genet Mol Res. 2015;14(2):4344-53. doi: 10.4238/2015.April.30.7.
24. Min Zhou 1, Yadi Zhang, Xulin Chen, Jianjun Zhu, Min Du, et al. PTEN-Foxo 1 signaling triggers HMGB1-mediated innate immune responses in acute lung injury. Immunol Res. 2015;62(1):95-105. doi: 10.1007/s12026-015-8639-z.

Figures

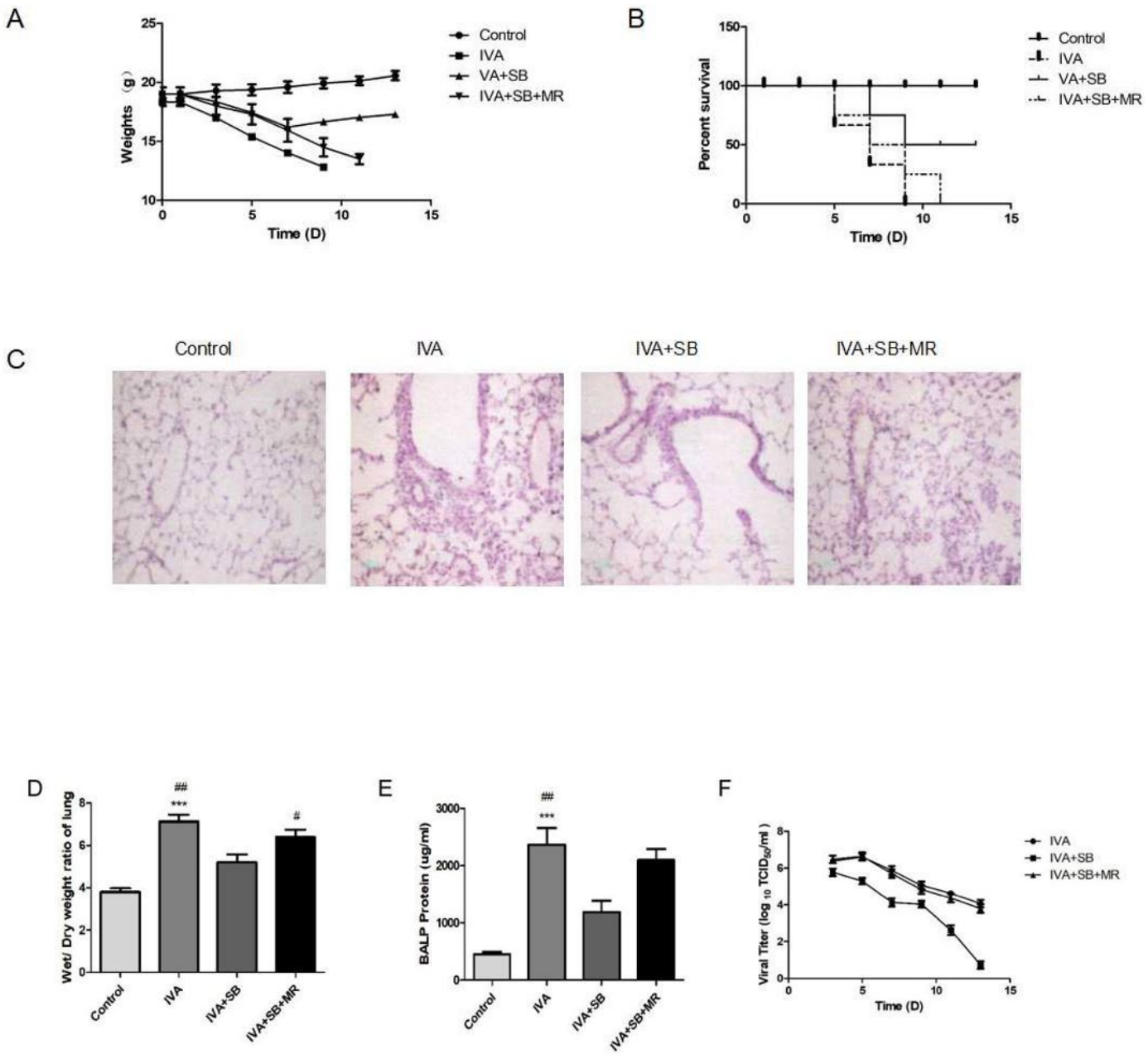

Figure 1

Respiratory symbiotic bacteria can reduce the infection ability of influenza virus. (A) Changes in weight of mice. (B) The percent survival of mice. (C) Histology of mice lung (x200). (D) Lung pathology wet/ dry weight. (E) The total protein concentrations in the BALF of infected mouse lungs. (F) Viral titer of lung. All data should be expressed as mean ± standard error. *P<0.05, **P<0.01, ***P<0.001 Vs Control; #P<0.05, ##P<0.01 Vs IVA+SB. IVA+SB: IVA+ symbiotic bacteria group; IVA+SB+MR: IVA + symbiotic bacteria + macrophage removal group.

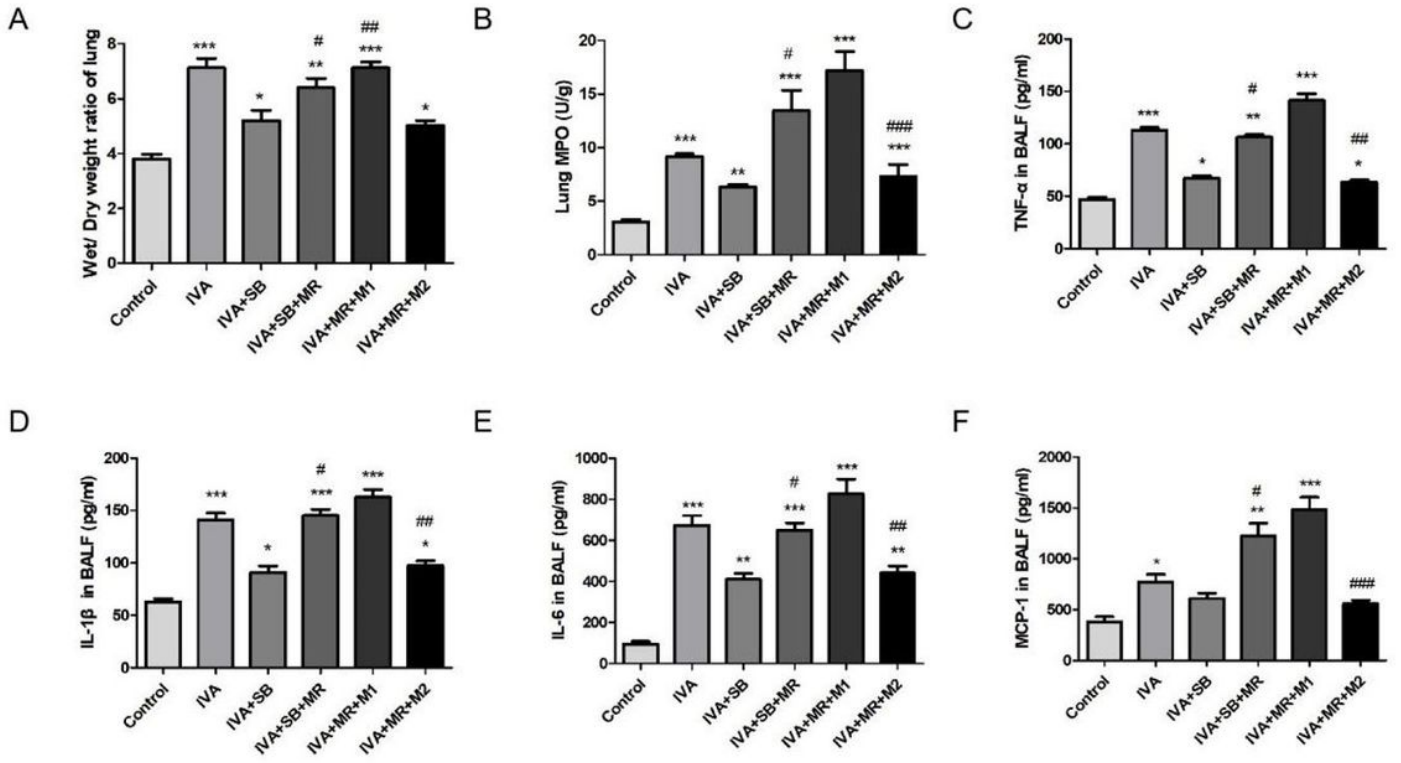

Figure 2

Type 1 alveolar macrophages aggravate the inflammatory infiltration of lung tissue in IVA mice. (A) Histogram of W/D ratio of each group of lungs. (B) Comparison of MPO activity in each group of lung tissues. (CF) ELISA method was used to determine pro-inflammatory cells TNF-a, IL- in mouse alveolar lavage fluid (BALF) 1β, IL-6 and MCP-1 levels. All data shall be expressed as mean ± standard error. *P<0.05, **P<0.01, ***P<0.001 Vs Control; #P<0.05, ##P<0.01, ###P<0.001 Vs IVA+SB.

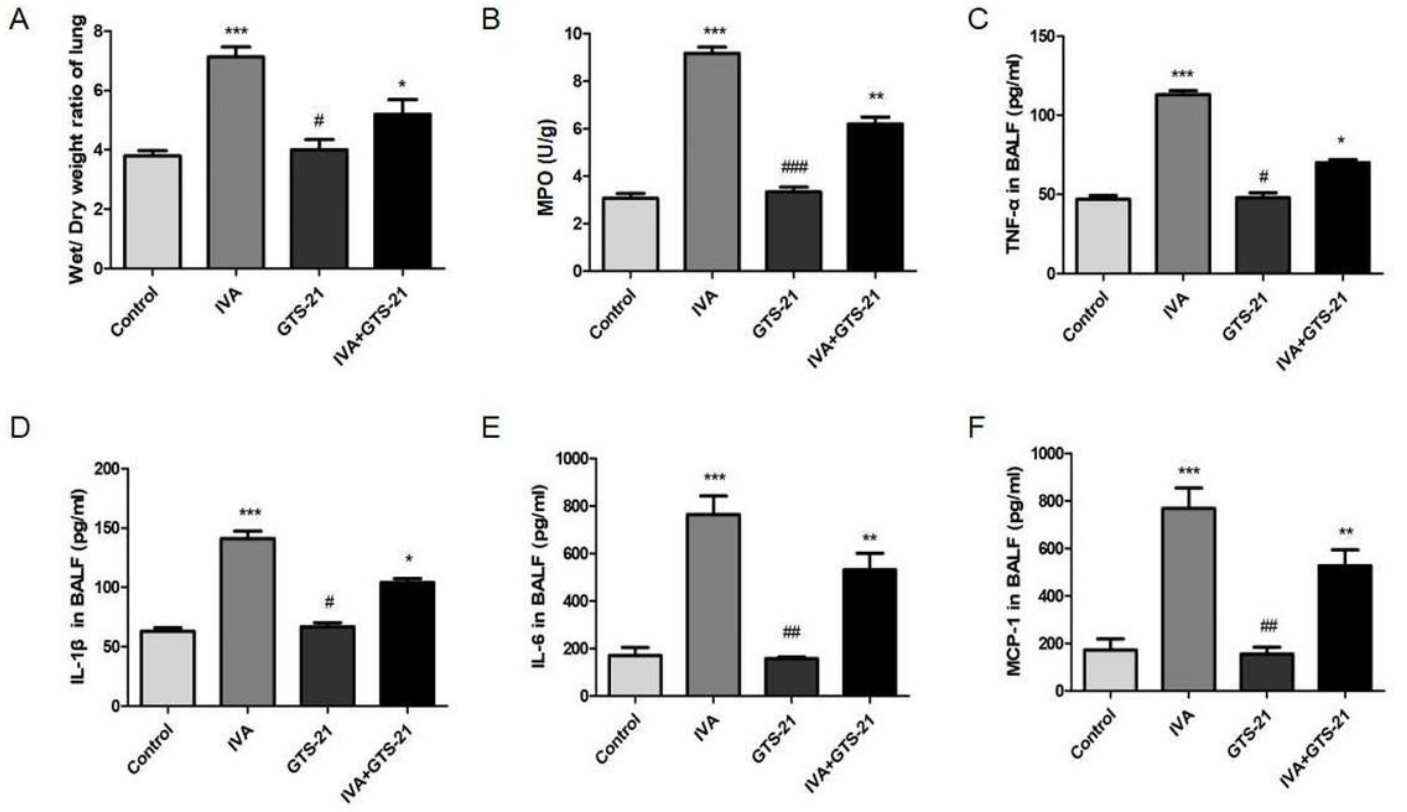

Figure 3

GTS-21 regulates lung inflammation response in mice with lung injury induced by IVA. (A) Histogram of W/D ratio of each group of lungs. (B) Comparison of MPO activity in each group of lung tissues. (CF) ELISA method was used to determine pro-inflammatory cells TNF-a, IL- in mouse alveolar lavage fluid (BALF) 1β, IL-6 and MCP-1 levels. All data shall be expressed as mean ± standard error. *P<0.05, **P<0.01, ***P<0.001 Vs Control; #P<0.05, ##P<0.01, ###P<0.001 Vs IVA+SB.

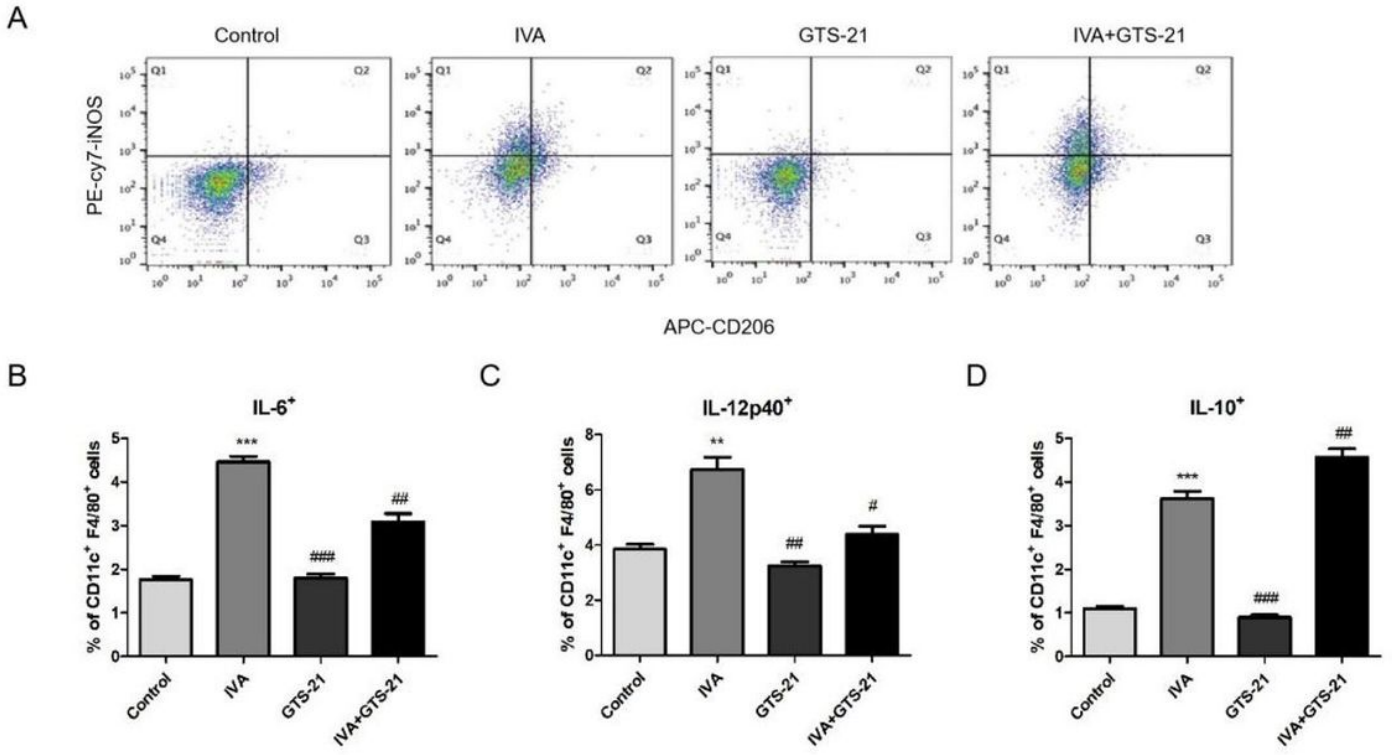

Figure 4

The effect of GTS-21 on the polarization of alveolar macrophages in mice with lung injury induced by IVA. (A) Flow cytometry was used to determine the percentage of AM cells expressing iNOS+ and CD206+ in each group of mice. (BD) GTS-21's effect on the expression level of AM molecules (IL-6, IL-12p40, IL-10) influences. All data shall be expressed as mean ± standard error. *P<0.05, **P<0.01, ***P<0.001 Vs Control; #P<0.05, ##P<0.01, ###P<0.001 Vs IVA.

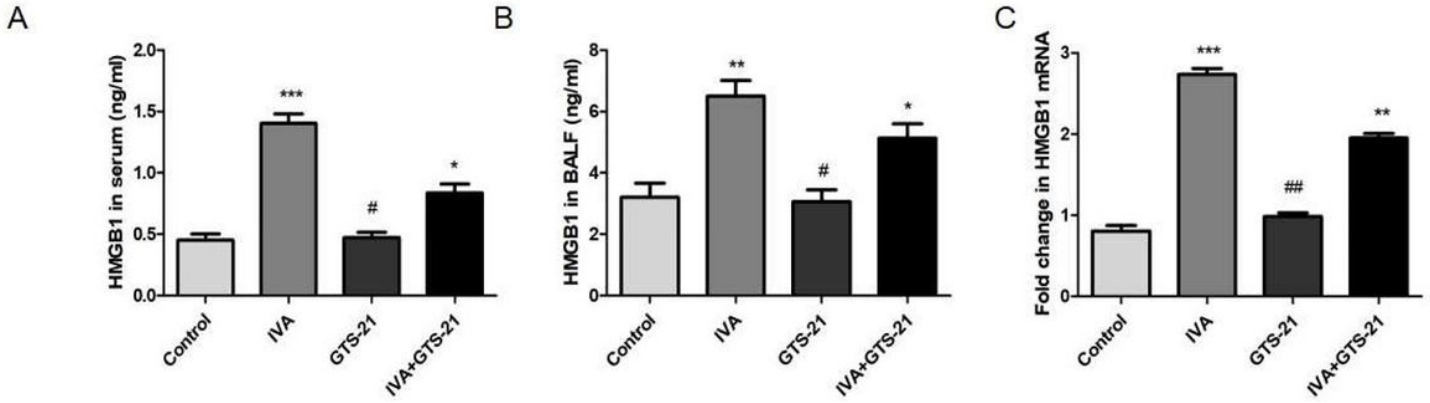

Figure 5

The effect of GTS-21 on HMGB1 in alveolar macrophages in mice with lung injury caused by IVA. (A-B) Comparison of the concentration of HMGB1 in mouse plasma and BALF in each group. (C) Comparison

of HMGB1 mRNA in AM in each group of mice. All data should be expressed as mean ± standard error. *P<0.05, **P<0.01, ***P<0.001 Vs Control; #P<0.05, ##P<0.01, ###P<0.001 Vs IVA.

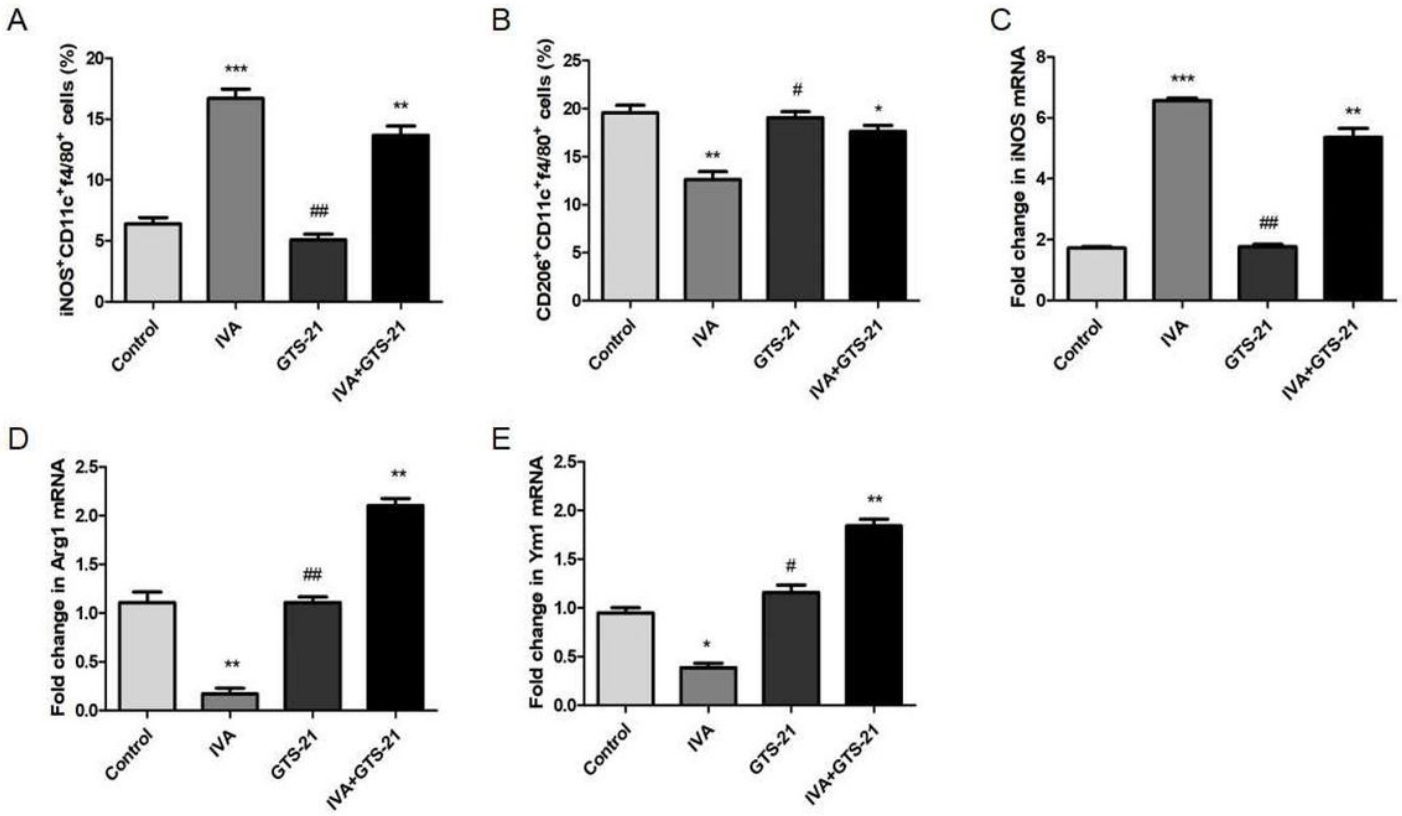

Figure 6

The effect of GTS-21 on the polarization of alveolar macrophages in mice with lung injury induced by IVA. (AB) Use flow cytometry to determine the percentage of cells expressing iNOS+ and CD206+ in each group of mice AM. (CE) 3) Use RT-PCR to determine the mRNA expression levels of iNOS, Argl, Yml in each group of mice AM. All The data shall be expressed as mean ± standard error. *P<0.05, **P<0.01, ***P<0.001 Vs Control; #P<0.05, ##P<0.01, ###P<0.001 Vs IVA.

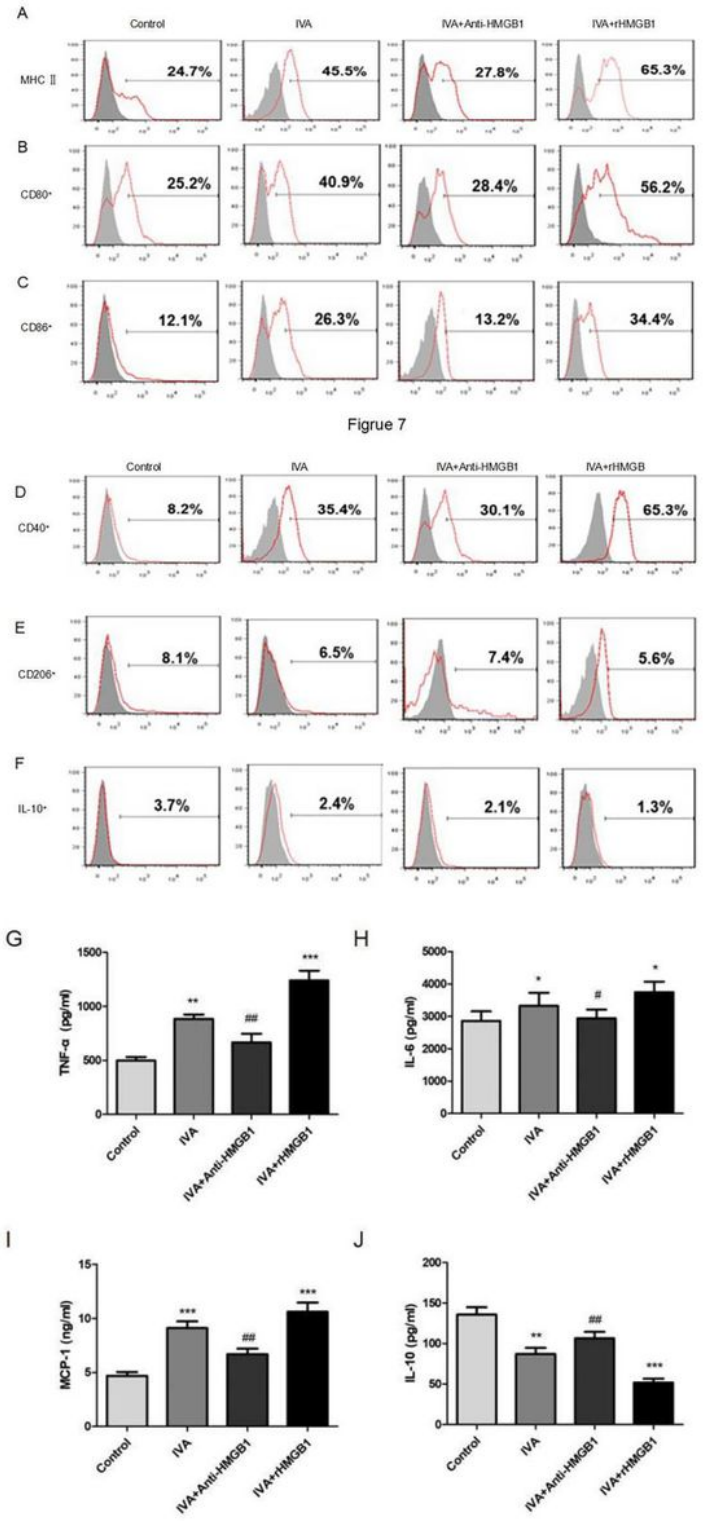

Figure 7

The effect of HMGB1 on the polarization of macrophages in mice with lung injury caused by IVA. (AF) Flow cytometry was used to detect the surface biomarkers related to M1 and M2 AMs after different interventions of rHMGBI and anti-HMGBI (MHCII, CD80, CD86, CD40, CD206, IL-10) expression levels and percentage changes. (GJ) ELISA was used to measure rHMGB1 and Anti-HMGBI intervention in the supernatant of macrophages derived from the bone marrow of IVA mice Changes in the expression levels

of cytokines (TNF-a, IL-6, MCP-1, 1L-10). All data shall be expressed as mean ± standard error. *P<0.05, **P<0.01, ***P<0.001 Vs Control; #P<0.05, ##P<0.01, ###P<0.001 Vs IVA.